Int. J. Morphol.,
42(5):1429-1438, 2024.

Morphological, Morphometrical and Histological Characteristics of Menisci in Domestic Cats (*Felis catus*)

Características Morfológicas, Morfométricas e Histológicas de los Meniscos en Gatos Domésticos (*Felis catus*)

Nur Izzati Inani Zabiddin[1]; Md Zuki Abu Bakar[1]; Mohd Akmal Mohd Noor[1]; Mohd Faizal Ghazali[2]; Chai Min Hian[2]; Dhiya Athirah Azman[1] & Siti Mariam Zainal Ariffin[1]

ZABIDDIN, N. I. I.; BAKAR, M. Z. A.; NOOR, M. A. M.; GHAZALI, M. F.; CHAI, M. H.; AZMAN, D. A.; ARIFFIN, S. M. Z. Morphological, morphometrical, and histological characteristics of menisci in domestic cats (*Felis catus*). *Int. J. Morphol., 42(5)*:1429-1438, 2024.

SUMMARY: This study aimed to investigate the morphological and morphometric features, as well as the histological composition of the medial and lateral menisci of domestic cats. A total of 180 menisci were obtained from 45 skeletally mature cat cadavers, followed by measuring the peripheral extension, width and thickness, circumference of the body and the body with horns, articulating height, and superior articulating length. A histological assessment was conducted to determine the meniscal cellularity and histomorphology. Each meniscus was evaluated in three regions (cranial horn, body, and caudal horn) and three zones (outer, middle, and deep). The proteoglycan content and collagen distribution were also examined. Overall, 62.2% of the medial meniscus displayed a crescentic shape, whereas 86.7% of the lateral meniscus exhibited a C-shaped configuration. The morphometric analysis revealed that the lateral menisci significantly differed ($P<0.05$) in circumference, thickness, width, and articulating height from the medial menisci. Despite cell density was not significantly different across the regions, the cellularity decreased from the outer zone to the deep zone of the menisci. Proteoglycan content was not significantly different in the various regions but was increased significantly ($P<0.05$) in the middle meniscal zone. Types I, II, and III collagens were distributed throughout the meniscal regions and zones. Type I collagen was abundant within the meniscus. In contrast, type III collagen is primarily localized in the middle zone. In conclusion, feline menisci exhibit morphometric variations and distinctive histological features, offering crucial insights for veterinarians and researchers.

KEY WORDS: Menisci; Morphometry; Histology; Stifle joint; Feline.

INTRODUCTION

The meniscus, a fibro cartilaginous structure, is located between the femoral and tibial condyles of the stifle joint. In their normal state, the menisci exhibit smooth, white, translucent, and glistening surfaces (Beale, 2009; Dyce *et al*., 2017). The menisci are connected to both the femur and tibia through the caudal and femoral ligaments of the lateral meniscus. There is an additional ligament that connects the lateral meniscus. The joint capsule attaches to the edge of each meniscus. The medial meniscus is less mobile since it is attached to the medial collateral ligament (Denny & Butterworth, 2000).

The menisci play a role in maintaining the normal mechanical functions of the stifle joint by managing forces such as tension, compression, and shear. These functions are important for protecting the articular cartilage and preventing joint disease (Messner & Gao, 1998). In addition, menisci are involved in weight-bearing activities and provide shock absorption, lubrication, and nutrition to the articular cartilage (Voss *et al*., 2017). The multi-functionality of the meniscus is supported by cellular activities, water, and the extracellular matrix (ECM), which includes collagen fibers and proteoglycans.

Multiple morphology and morphometric studies of the meniscus have been previously conducted both in humans and animals (Pauli *et al*., 2011, Braz & Silva, 2012, Takroni *et al*., 2016, Gupta *et al*., 2022). Nevertheless, literature reporting the comprehensive morphology of the meniscus in felines is relatively lacking. In 1978, O'Connor

[1] Department of Veterinary Preclinical Sciences, Faculty of Veterinary Medicine, Universiti Putra Malaysia, Serdang, Selangor, Malaysia.
[2] School of Animal Science, Aquatic Science & Environment, Faculty of Bioresources and Food Industry, Universiti Sultan Zainal Abidin, Besut, Terengganu, Malaysia.
FUNDED: This study was funded by Geran Inisiatif Putra Muda (GP-IPM) (Project code: GP-IPM/2022/9714600).

Received: 2024-06-13 Accepted: 2024-07-12

& McConnaughey reported that the shape disparity of the feline medial meniscus was less as compared to the lateral meniscus. Prosé (1984) also found that feline menisci generally exhibit a C-shaped configuration, with the lateral meniscus tending to be smaller than the medial meniscus. A more recent article by Chakravarthy & Khanday (2018) highlighted the importance of identifying the variations in the dimensions of the lateral and medial menisci in predicting the occurrence of meniscal injuries.

Briefly, various collagen types (type I, II, III, IV, and V) can be found within a normal meniscus, with collagen type I constituting 90 % of the collagen composition (McDevitt & Webber, 1990). However, the distributions of the collagen types vary across different regions of the meniscus, depending on the specific functional requirements and the biomechanical characteristics of the meniscus regions (Vanderploeg *et al.*, 2012). Meanwhile, proteoglycans are an integral part of the ECM that helps maintain the structure and function and facilitate water-retention properties of the meniscus during compression. Studies have demonstrated a regional variation in the proteoglycan distribution within the porcine menisci, where the proportion of proteoglycan was greater in the inner two-thirds region in comparison to the outer one-third region of the menisci (Scott *et al*., 1997; Nakano *et al*., 2005).

To date, the specific histological composition of the feline meniscus has not been fully elucidated. Hence, understanding the histological composition of the feline meniscus could provide valuable insights into the distinctive characteristics and adaptations of this structure in feline species. Furthermore, improving the knowledge in this area holds promise for a better solution in addressing meniscus-related orthopedic conditions among felines. Thus, this study aimed to determine the morphology and morphometric characteristics of the medial and lateral meniscus in domestic cats, including the histological composition of the meniscus across regions and zones. We hypothesized that feline menisci are heterogeneous, reflecting variations in the morphology, morphometric measurements, and compositional and structural organization of the meniscus on a regional and zonal basis.

MATERIAL AND METHOD

Cat cadavers. The study involved meniscal tissue samples from 45 skeletally adult cat cadavers that had been euthanized for reasons unrelated to this study and were brought to the Faculty of Veterinary Medicine, Universiti Putra Malaysia. According to the Malaysian Code of Practice for the Care and Use of Animals for Scientific Purposes (MYCODE), tissue samples from deceased animals do not require local Ethics Committee approval. The inclusion criteria were mature skeletal age (2 years and above), healthy stifle joints (no tibiofemoral osteoarthritis, no cranial cruciate ligament rupture), and healthy meniscus (no tears or degeneration). The mean age of all the cat cadavers was 2.5 years (18 months to 3 years). Thus, a total of 180 menisci (90 each for medial and lateral menisci) from 45 cat cadavers were evaluated. The stifle joints were examined within 24 hours post-mortem. Furthermore, each meniscus (medial and lateral menisci) was grossly examined and digitally photographed.

Morphological assessment of feline menisci. The shape of the menisci was observed in situ and categorized either as incomplete discoid, complete discoid, crescentic-shaped, sickled-shaped, C-shaped, sided V-shaped, or sided U-shaped (Kale *et al*., 2006).

Morphometric assessment of feline menisci. The lateral and medial meniscal circumference, width, thickness, superior articulating length, and articulating height were measured according to Takroni *et al*. (2016), and Subramanian & Balakrishnan (2023).

Circumference. The inner and outer circumferences of the lateral and medial menisci were quantified using molded and flexible tape. The outer and inner circumferential measurements were made along the outer and inner perimeters of each border, from the end of the cranial horn to the end of the caudal horn (Fig. 1a).

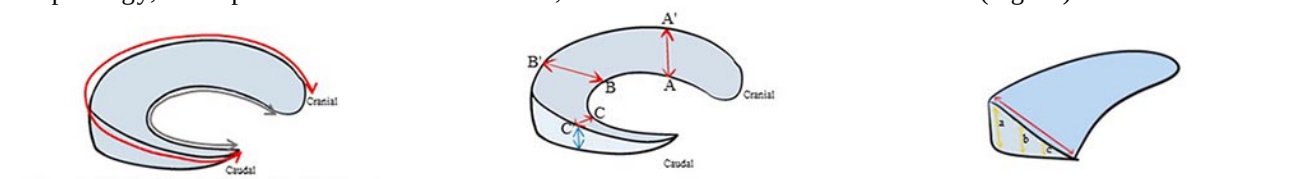

A The outer (red double curved arrow) and the inner (grey double curved arrow) circumferences measurements of the menisci.

B The width (red double headed arrows) and the thickness (blue double headed arrows) measurements of the menisci.

C The superior articulating length (red double headed arrow) and the articulating height (yellow double headed arrows) measurements of the menisci.

Fig. 1. Illustration (a) presents the outer and inner circumferential measurements of the menisci. (b) The width of the menisci was measured at three distinct points: A-A' (cranial third), B-B' (middle third), and C-C' (caudal third). The thickness of the menisci was measured at the three points (A', B', and C'). (c) The superior articulating height was measured from the highest point on the outer edge to the lowest point on the inner edge in the middle third of the body. The articular height was calculated by dividing the superior articular length into three equally measured points: a (outer), b (middle), and c (deep). The measurement values were reported in millimeters (mm).

Width and thickness. The inner circumferential length was divided into three points A, B, and C. Similarly, the outer circumferential length was separated into three points A', B' and C'. The points were joined from the innermost to the outer edges (i.e. A-A', B-B', and C-C'), and the width of the meniscus at these points was measured using a digital Vernier caliper. The thickness was assessed by positioning the digital caliper vertically between the femoral and tibial surfaces of the menisci at specific width points along the outer border. The menisci were then divided into three parts (Fig. 1b).

Superior articular length and articular height. The superior articular length was determined by measuring from the highest point on the outer edge to the lowest point on the inner edge in the middle third of the body. The articular height was calculated by dividing the superior articular length into three equally measured points: a (outer), b (middle), and c (deep). One jaw of the digital caliper was positioned on the femoral surface, and the other was placed beneath the flat bottom surface. Both jaws were then systematically moved to four locations at three predetermined distances (Fig. 1c).

Tissue Processing and Staining. The meniscal samples were fixed in 10 % buffered formalin. The formalin-fixed menisci were processed using a preset program on a tissue processor for 15.5 h. Subsequently, the treated tissues were embedded in paraffin wax. The horizontal and radial cross-sections of the paraffin-embedded menisci were sectioned at 5.0 μm using a Jung Multicut RM2045 microtome and affixed onto the glass slides. The slides were dried on HI 1220 Leica hot plate at 40 °C for 3 days to remove moisture.

Haematoxylin and eosin (H&E) staining. All sections were routinely stained with H&E for cell density assessment. The sections were deparaffinized by immersion in xylene and rehydrated with 100 %, 95%, and 80 % ethanol and distilled water. The slides were immersed in hematoxylin for five minutes and then rinsed with distilled water for 10 seconds. Subsequently, the slides were briefly dipped in acid ethanol for 10 seconds to remove excess hematoxylin and enhance cellular differentiation, followed by rinsing with tap water. Subsequently, each slide section was counterstained with eosin for 30 seconds and subsequently dehydrated with 70 %, 80 %, 95 %, and 100% ethanol. The sections were cleared in xylene and mounted with DPX mountant.

Safranin O and fast green staining. In this study, Safranin O staining (Solarbio® Life Sciences, Beijing, China) was used to determine the proteoglycan distribution in the meniscal regions and zones. Firstly, the sections were deparaffinized and rehydrated. Next, the sections were immersed in Weigert's hematoxylin solution for five minutes and then rinsed with distilled water for 10 minutes. After that, the sections were stained with the fast green solution for 5 min and rinsed with weak acid for 12 s. The slides were then air-dried and stained with Safranin O staining solution for 5 min. Each stained slide was dehydrated at 90 % and 100 % for 1 min and cleared in xylene. Lastly, the slides were mounted with the DPX mountant.

Picrosirius red staining. In the present study, Picrosirius Red staining (Solarbio® Life Sciences, Beijing, China) was used to identify the collagen types I and III that are present in the sections. The special dye picrosirius red can enhance the natural birefringence of the collagen when exposed to polarized light. Firstly, the sections were deparaffinized and rehydrated before being stained with hematoxylin solution for 10 min. The stained sections were rinsed in distilled water for 15 s to remove excess stain. Next, the sections were rinsed with tap water for 10 min before being immersed and stained with Sirius Red staining solution for 30 min. The stained sections were then rinsed gently in tap water to remove excess stains. Thereafter, the sections were dehydrated in 75 % ethanol, followed by 95 % ethanol, and absolute ethanol (I) with each procedure lasting three seconds. The sections were then dehydrated using absolute ethanol (II) for one minute, before clearing in xylene and mounted with DPX the mountant.

Immunohistochemistry. The sections were deparaffinized and rehydrated, followed by a five-minute wash in phosphate-buffered saline (PBS). To retrieve the antigen, the sections were immersed in a heated sodium citrate buffer with a pH of 6.0 for five minutes. The endogenous peroxidase activity was inhibited by submerging the sections in a 1.0 % hydrogen peroxide solution in methanol for 30 min, followed by two rounds of five-minute rinses using PBS. Non-specific binding was mitigated by a 30-min block with supplemented blocking (Bovine Serum Albumin; BSA). Subsequently, the sections were incubated with a Polyclonal Antibody (rabbit anti-collagen II) (1:200; bs-0709R, Bioss, China) diluted in primary antibody diluent at room temperature for two hours. Following two rounds of five-minute rinses in PBS, the sections underwent a 30-min incubation with the secondary antibody (horse anti-rabbit), which was diluted in a secondary antibody diluent. After two five-minute washes with PBS, the sections were incubated with peroxidase-conjugated avidin for 30 min. Following two sets of five-minute rinses using PBS, the visualization of the antigen-antibody complex was achieved through DAB. Counterstaining with hematoxylin and subsequent washing in running tap water were also conducted. Finally, the sections underwent dehydration, were clarified using xylene, and then mounted with DPX. Non-specific staining was evaluated by incubating replicate sections with nonimmune antibodies.

Histological assessments and scoring. All sections were analyzed and imaged using a light microscope (Motic BA410 with an attached Moticam Pro 285A camera). The meniscal sections stained with picrosirius red were assessed separately under polarized light (Motic BA410e Polarize Analyze Filter).

The cell density was quantitatively analyzed as described by Fedje-Johnston *et al*., (2021). Images of sections stained with H&E were acquired at 100X to detect cell nuclei. For this assessment, five images were captured from each region (cranial third, middle third, and caudal third) and zone (outer, middle, and deep), which were then analyzed by ImageJ software. The multipoint tool was used to mark the cell nuclei. The cellular density was determined by adding up the cell counts and dividing the total by the tissue area, which was measured at 1.50 square millimeters. This approach was employed to establish the cell density in various regions and zones of the meniscus.

Color thresholding was used to measure the intensity of stain uptake for proteoglycans (red stain, Safranin O), collagen type I (green stain) and III (orange stain) (picrosirius red) and collagen type II (IHC) using the software ImageJ. The overall area of the stained sections was calculated by dividing the positive staining cell by the total cells in each selected area within the respective region or zone (Fedchenko & Reifenrath, 2014). The value obtained was expressed as percentages. The staining intensity was graded 0 (non-staining), 1 (1-25 %, weak staining), 2 (26-50 %, moderate staining), or 3 (>50 %, strong staining).

Statistical analysis. A descriptive statistical analysis of the morphometric parameters of the lateral and medial menisci was performed. The mean ± standard deviation (SD) was used to express the cellular density and morphometric data. A paired t-test was applied to compare the means between the lateral and medial menisci within the identical joint. One-way analysis of variance (ANOVA) was performed to compare the cellular density among meniscal zones and regions. Tukey's multiple comparison test was then used to assess any significant difference between each group. The Kruskal–Wallis test was conducted to detect variations in the localization and distribution of proteoglycans and collagen across meniscal regions and zones. Dunn's multiple comparison test was used as a *post-hoc* test to assess the difference between each group. For statistical analyses, a level of significance was set at $P<0.05$. The statistical analysis was conducted using GraphPad Prism for Windows, version 9.

RESULTS

Morphological assessment of feline menisci. A total of 180 menisci from 45 cats were evaluated, of which 90 each were medial and lateral menisci. All the menisci were grossly normal, smooth, and glistening upon examination. Three morphological variations of the medial menisci were identified. Overall, the predominant morphology identified in the medial meniscus was crescentic-shaped (62.2 %; 56/90), followed by discoid-shaped (22/90; 24.4 %) and C-shaped (12/90; 13.3 %). Only two morphological variations were found in the lateral meniscus: 86.7 % (78/90) of the meniscus was C-shaped, and 13.3 % (12/90) was crescentic-shaped (Fig. 2).

Morphometric assessment of feline menisci. The average outer circumference was 23.28±1.91 mm in the lateral menisci and 22.29±2.50 mm in the medial menisci, whereas the inner circumference was 13.05±1.96 mm in the lateral menisci and 12.20±2.41 mm in the medial menisci. The outer (P=0.0031) and inner (P=0.0101) circumferences of the lateral menisci were significantly greater than those of the medial menisci (Table I).

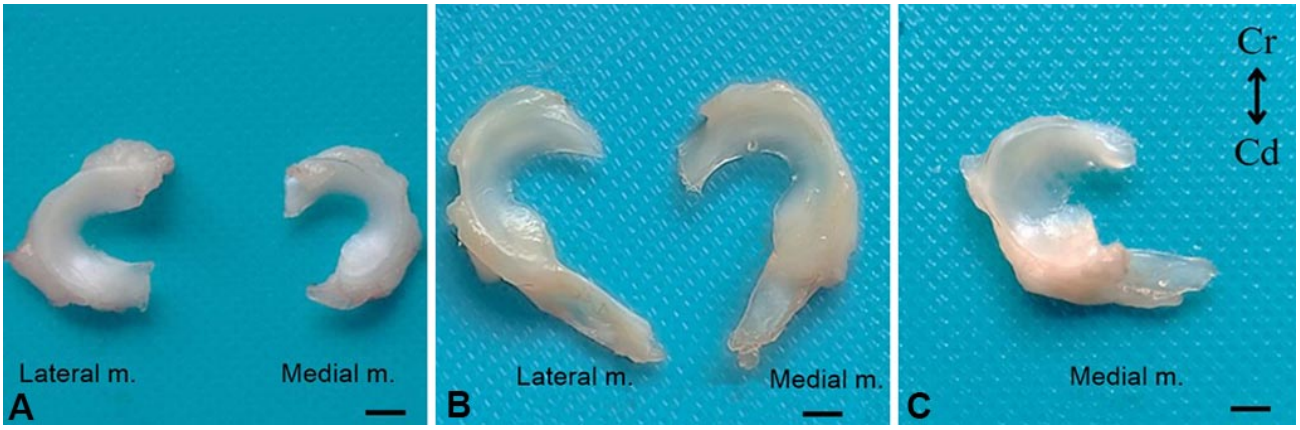

Fig. 2. Gross morphology of the lateral and medial menisci (m.) shows (a) C-shaped, (b) crescentic-shaped, and (c) discoid-shaped. Cr: cranial; Cd: caudal. Scale bar = 5 mm.

Table I. Morphometry measurement of the lateral and medial menisci.

	Lateral meniscus (n=90)	Medial meniscus (n=90)
Circumference		
Outer	23.28 ± 1.91**	22.29 ± 2.50
Inner	13.05 ± 1.96*	12.20 ± 2.41
Width		
Cranial third	3.61 ± 0.43	3.71 ± 0.63
Middle third	3.90 ± 0.52**	3.62 ± 0.70
Caudal third	3.21 ± 0.45	3.18 ± 0.62
Thickness		
Cranial third	2.11 ± 0.35	2.25 ± 0.46*
Middle third	1.76 ± 0.34***	1.35 ± 0.28
Caudal third	2.05 ± 0.45***	1.47 ± 0.40
Articular height		
Outer	1.76 ± 0.36***	1.35 ± 0.29
Middle	0.65 ± 0.16***	0.53 ± 0.12
Deep	0.30 ± 0.12**	0.25 ± 0.10
Superior articulating length	3.91 ± 0.51**	3.65 ± 0.70

Data presented as mean ± SD. Statistically significant are denoted by asterisks (*).*** represents $P<0.001$; **represents $P<0.01$ and *represents $P<0.05$.

The width and thickness of the meniscus were measured in three different regions; cranial third, middle third, and caudal third, with corresponding values of 3.61±0.43 mm, 3.90±0.52 mm, and 3.21±0.45 mm for the lateral menisci and 3.71±0.63 mm, 3.62±0.70 mm and 3.18±0.62 mm for the medial menisci, respectively (Table I). The middle (P=0.0036) third of the lateral menisci was significantly wider than the medial menisci. The cranial, middle, and caudal third thicknesses were 2.11±0.35 mm, 1.76±0.34 mm, and 2.05±0.45 mm in the lateral menisci, and 2.25±0.46 mm, 1.35±0.28 mm and 1.47±0.40 mm in the medial menisci, respectively. The cranial third of the medial menisci was significantly thicker ($P<0.05$) than the cranial third of the lateral menisci ($P=0.0224$) (Table I). However, the thickness of the medial menisci decreased significantly relative to that of the lateral menisci as it extends caudally.

The articulating height of the lateral and medial meniscus was measured at the outer, middle, and deep parts (Table I). The articulating height of the lateral menisci in all areas was significantly greater than that of the medial menisci ($P<0.001$). The superior articulating length of the lateral menisci (3.91±0.51 mm) was significantly longer than that of the medial menisci (3.65±0.70 mm) ($P=0.0049$).

Regional and Zonal Histological Composition of Feline Menisci

Cellular density. The cell density was not significantly different across the meniscal regions ($P=0.6592$) (Fig. 3a). Nevertheless, the cell density was significantly greater in the outer zone (999.8±283.1 cells/mm^2) than in the middle (873.0±309.0 cells/mm^2) and deep (776.9±182.7 cells/mm^2) zones (P=0.0205) (Fig. 3b). The cellularity gradually reduces while moving from the outer to the deep zones of the meniscus.

Proteoglycan. Proteoglycan in each region and zone of the meniscus was evaluated by examining the intensity of safranin O staining (Fig. 4a). The staining depicts a consistent percentage of positively-stained cells ranging from 1-28% (Score 1 and 2). No significant difference was observed in the Safranin O intensity score between the cranial third, middle third, and caudal third regions of the menisci ($P=0.4202$) (Fig. 4b). In contrast, the middle zone depicted the highest positively-stained cells with a percentage >50% (Score 3). Hence, a greater intensity of Safranin O staining was evident in the middle zones (P=0.0012) than in the outer and deep zones (Fig. 4c).

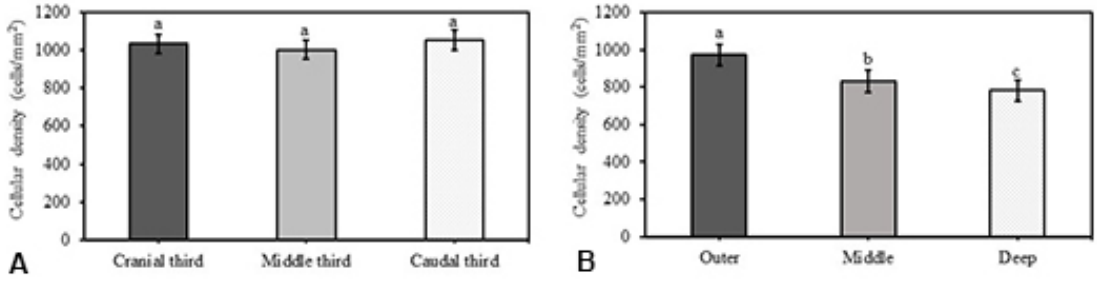

Fig. 3. Cellular density measurements in different meniscal regions (a) and zones (b). There is no significant difference in the mean cellular density between the cranial third, middle third, and caudal third regions of the menisci ($P=0.6592$). The cell density is significantly greater in the outer zone (999.8±283.1 cells/mm^2) than in the middle (873.0±309.0 cells/mm^2) and deep (776.9±182.7 cells/mm^2) zones ($P=0.0205$). Each bar denotes the mean ± SD (n=180).

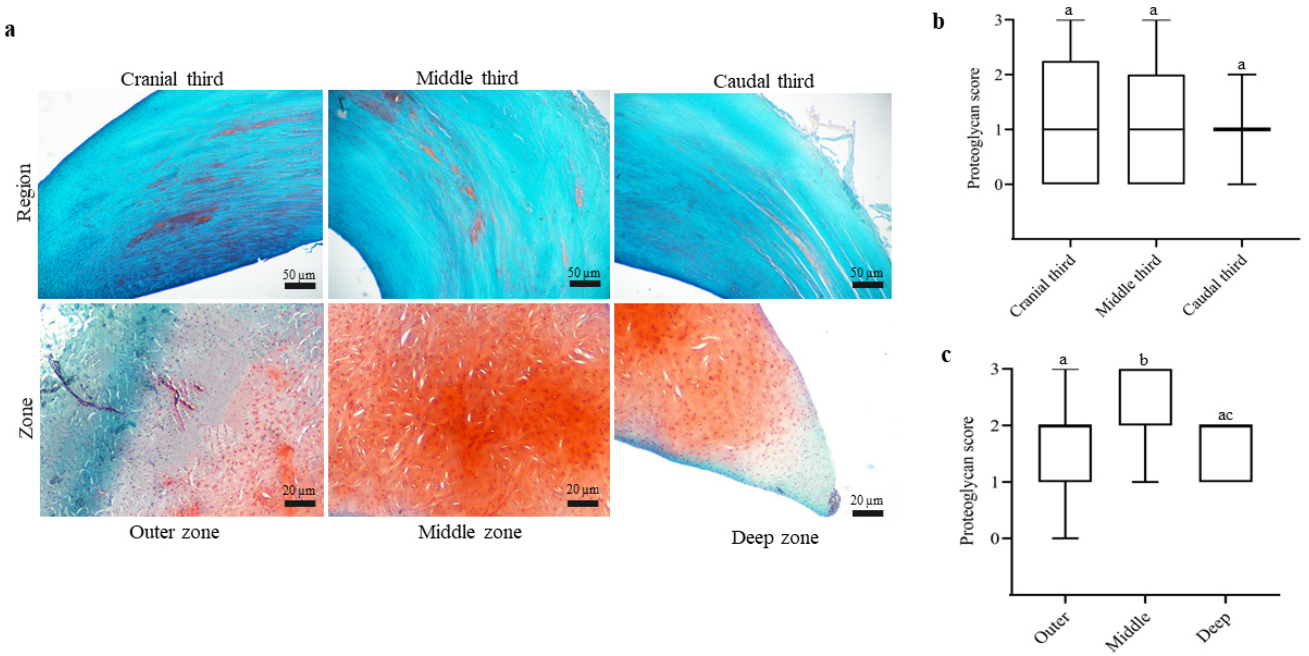

Fig. 4. (a) Safranin O staining for proteoglycans in meniscal tissue. Proteoglycan within the menisci were stained red. In contrast, fibrocartilage was stained blue-green coloration, allowing for the distinction and visualization of the fibrous components. Examples of Safranin O staining in the cranial third, middle third, and caudal third for the horizontal section of the meniscal region taken at 40X magnification. Additionally, examples of Safranin O staining in the outer zone, middle zone, and deep zone for the cross-section of the meniscus are taken at 100X magnification. The Safranin O staining in the middle zone exhibited a strong and intense red coloration, suggesting a high concentration of proteoglycans. The box plot graphs show variations in proteoglycan scores within different regions (b) and zones (c). Data presented as median. Data with different superscripts indicating significant differences (n=180).

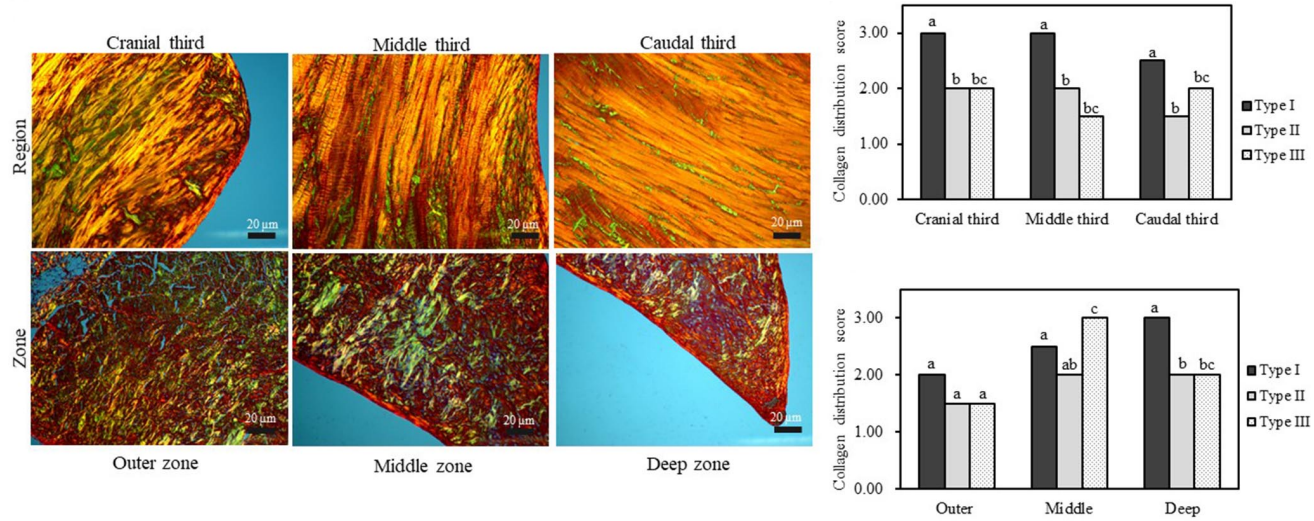

Fig. 5. (a) Picrosirius red staining, observed under polarized light at 40X magnification, revealed the distinct distribution of type I collagen (depicted in yellow-red) and type III collagen (displayed in green) within various regions and zones of the menisci. The representative micrographs show a score of 3 for collagen type I staining in the cranial third, middle third, and caudal third of the meniscal regions. The distribution of collagen type III was notably prominent within the middle zone (Score 3). The bar graphs show variations in collagen distribution scores among types I, II, and III within different regions (b) and zones (c). Data presented as median. Data with different superscripts indicating significant differences (n=180).

Collagen. Distinct levels of collagen types I, II, and III were observed in various meniscal regions and zones, as evident in Figures 5 and 6. Collagen type I reflected the highest collagen distribution score across the meniscal regions, with a percentage ranging from 1-80% and classified under the scores 1 to 3 (Fig. 5b). However, collagen types II and III

were not as abundant as type I. The positively-stained collagen types II and III ranged from 1-40% (Score 1 to Score 2) (Fig. 5b). The result depicts a significant abundance of type III collagen within the meniscal middle zone, with a percentage ranging from 40-60% (Fig. 5c). When observed under polarized light, type I collagen was presented as fibers in shades of yellow-red, whereas type III collagen appeared as fibers with a green hue (Fig. 5a).

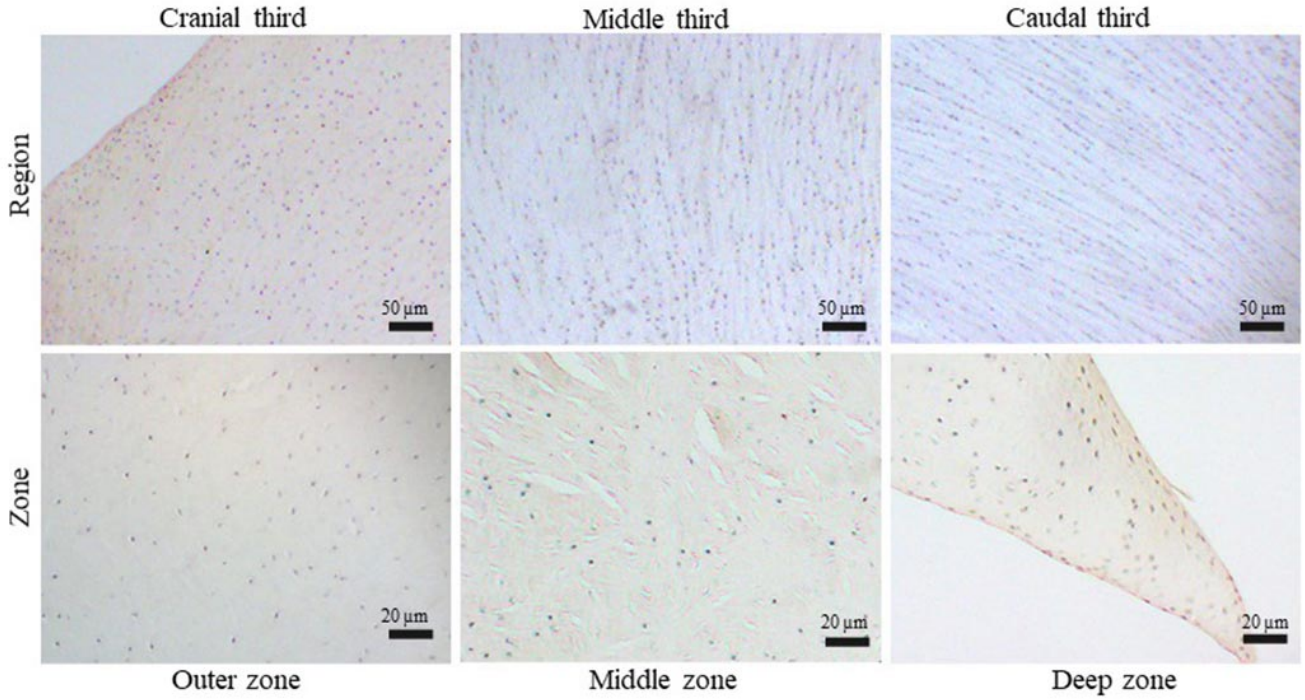

Fig. 6. Immunohistochemical staining of collagen type II in different regions and zones of the menisci. Representative micrographs show an IHC score of 3 in the cranial third and deep zone of the menisci. Meniscal regions: 40X magnification; meniscal zones: 100X magnification.

DISCUSSION

The present study investigates the morphological and morphometric characteristics of the lateral and medial menisci of domestic cats. These findings challenge the conclusions drawn by previous research, specifically the work of Prose in 1984, which reported that the feline meniscus exclusively exhibits a crescentic shape. Our study suggested that this may not be the case given the more diverse range of shapes observed in the feline meniscus. Parson (1899) reported that mammalian menisci have the same semilunar shape regardless of their walking style and size. The shape of the meniscus can vary among different animal species. Abumandour *et al*. (2019), reported the meniscal morphology in various animals. The medial meniscus in donkeys usually has a crescentic shape. Nonetheless, in goats, the meniscus demonstrated a semi-circular shape, whereas both the medial and lateral menisci depicted were C-shaped in dogs. The variations in meniscal morphology among various species of animals may stem from evolutionary adaptations, biomechanics, and specific joint requirements.

The present study revealed that the medial meniscus exhibited a greater morphological variation compared to the lateral meniscus. This finding contradicts that of O'Connor & McConnaughey (1978), who reported fewer shape variations in the medial meniscus compared to the lateral meniscus. Meanwhile, variants of the discoid meniscus have not been described in cats. We found that 22/90 (24.4%) of the medial menisci in the present study were discoid, which is a rare anatomic structure in dogs but relatively common in the human pediatric population (Kim *et al*., 2016). The discoid-shaped meniscus in humans is reported as a morphological anomaly, which stems from the failure to absorb the inner part of the menisci during embryonic development (Kim *et al*., 2020). Meanwhile, the gross examinations conducted in the current study revealed that the discoid meniscus covers the tibial plateau circularly. The discoid meniscus is also thicker than the crescentic and C-shaped menisci. In comparison to the non-discoid-shaped meniscus, the risk of injuries is higher in the discoid meniscus, given its greater susceptibility to compression and

more likely to be stuck between the femoral condyle and tibial plateau, leading to tears and damage (Johnson & Steinbach, 2005).

The thickness of the meniscus is one of the factors that influence the ability of the meniscus to resist compression, sheer forces, and torsional loads during physical activities such as jumping, running, or sudden changes in direction. Previous studies have suggested that the increased incidence of damage observed in the feline medial meniscus is possibly due to the distinct anatomical features of the medial meniscus (Beale, 2009; Ruthrauff *et al*., 2011; Koch & Kornmayer, 2023). Specifically, the medial meniscus was identified to be more vulnerable to trauma and injury due to its thinness and decreased mobility (Braz & Silva, 2010).

This study revealed that the meniscal articulating height increased at the outermost edge, gradually tapering toward the innermost edge. This finding supports the report by Takroni *et al*. (2016), who demonstrated that the menisci are a wedge-shaped structure. Furthermore, we found that the superior articulating length of the lateral menisci was longer in comparison to the medial menisci. According to Fox *et al*. (2012), a longer articulating length might enhance the shock absorption ability of menisci and help to reduce impact forces during weight-bearing activities such as walking, running, and jumping. Furthermore, an increased articulation length may facilitate a more efficient distribution of forces and loads on the stifle joint, thereby reducing the stress on the articular cartilage and supporting bone structures (Fox *et al*., 2012). In addition, the present findings corroborate the reports suggesting that lateral compartment stifle osteoarthritis in cats is less severe as compared to the medial compartment, possibly due to the efficient load distribution in the lateral meniscus region (Bennett *et al*., 2012; Leumann *et al*., 2019). Nonetheless, additional research is required to elucidate the underlying mechanisms regarding the differences in load distribution between the medial and lateral compartments of the stifle joint in felines.

Another important finding was the fact that the density of the meniscal cells was always highest in the outer zone while depicting a decreasing trend in the middle and deep zones of the meniscus. The differences in meniscal cell density may arise from the vascularity of the different meniscus zones. An earlier study reported that the outer zone of the meniscus is more vascularized than the inner zone (O'Connor & McConnaughey, 1978). Cengiz *et al*. (2015), also suggested that greater vascularity in the outer zone increases blood supply, nutrients, and oxygen, creating a more favorable environment for cells. Furthermore, the varying cell density across the meniscal zones of the meniscus may play a role during the injury healing processes. The higher cell density in the outer zone suggested that the cells may have a greater intrinsic repair capacity; hence, more likely to heal faster than the middle and deep zones (Chevrier *et al*., 2009; Yan *et al*., 2021).

In the present study, a high intensity of proteoglycan staining was found within the middle zones of the feline menisci, as shown in Figure 4. This finding is consistent with previous studies investigating the distribution of proteoglycans in the healthy meniscus of various species. For instance, Nakano *et al*. (2005), demonstrated that the inner zone of the menisci of porcine has the highest concentration of proteoglycan. Furthermore, previous studies conducted in humans (Nerurkar *et al*., 2011), canines (Adams & Muir, 1981), rabbits, and sheep (Chevrier *et al*., 2009) also reported a higher concentration of proteoglycans in the middle and deep zones of the menisci. This concentration imparts the ability of the middle and deep zones to withstand substantial compressive loads while maintaining stiffness.

Type I collagen is the most abundant collagen and is ubiquitous in menisci. This observation is consistent with earlier research conducted in cattle, pigs, dogs, and humans (Eyre & Wu, 1983; McDevitt & Webber, 1990; Kambic & McDevitt, 2005). Type I collagen I imparts tensile strength to the meniscus, allowing it to withstand stretching forces (Starke *et al*., 2018). Although types II and III collagens are also present in the meniscus, they are not as abundant as collagen type I. Notably, type III collagen is abundant in the middle zone of the meniscus (Fig. 5). Collagen type II helps in resisting compressive forces, while collagen type III contributes to the flexibility and resilience of the meniscus, particularly in regions characterized by a combination of tensile and compressive forces (Wang *et al*., 2020). Collagen type III is predominantly located in the transition zone between the outer and inner zones of the meniscus (Wang *et al*., 2020). Using the picrosirius red staining method under a light-polarized microscope not only improved the visual distinction between collagen types I and III in feline meniscal tissue but also enabled two-dimensional assessments (Liu *et al*., 2021). This was achieved by determining the proportion of distinct color areas using morphometric image analysis. Nevertheless, understanding the complex three-dimensional orientation of collagen fibers in the meniscus still demands additional research.

CONCLUSION

There were variations in morphology and morphometry between the lateral and medial menisci of domestic cats. The histological composition of the meniscus reveals the variation in the distribution of cellular density,

proteoglycan, and collagen fibers. The results of this study provide valuable information and contribute to a better understanding of feline meniscal anatomy and its structure-function relationship.

ZABIDDIN, N. I. I.; BAKAR, M. Z. A.; NOOR, M. A. M.; GHAZALI, M. F.; CHAI, M. H.; AZMAN, D. A.; ARIFFIN, S. M. Z. Características morfológicas, morfométricas e histológicas de los meniscos en gatos domésticos (*Felis catus*). *Int. J. Morphol., 42(5)*:1429-1438, 2024.

RESUMEN: Este estudio tuvo como objetivo investigar las características morfológicas y morfométricas, así como la composición histológica de los meniscos medial y lateral de gatos domésticos. Se obtuvieron un total de 180 meniscos de 45 cadáveres de gatos esqueléticamente maduros, y luego se midió la extensión periférica, el ancho y el grosor, la circunferencia del cuerpo y el cuerpo con cuernos, la altura de las articulaciones y la longitud de las articulaciones superiores. Se realizó una evaluación histológica para determinar la celularidad meniscal y la histomorfología. Cada menisco se evaluó en tres regiones (asta craneal, cuerpo y asta caudal) y tres zonas (externa, media y profunda). También se examinaron el contenido de proteoglicanos y la distribución de colágeno. En general, el 62,2 % del menisco medial mostró una configuración en forma de media luna, mientras que el 86,7 % del menisco lateral exhibió una configuración en forma de C. El análisis morfométrico reveló que los meniscos laterales diferían significativamente (P<0,05) en circunferencia, grosor, ancho y altura de los meniscos mediales. A pesar de que la densidad celular no fue significativamente diferente entre las regiones, la celularidad disminuyó desde la zona exterior a la zona profunda de los meniscos. El contenido de proteoglicanos no fue significativamente diferente en las distintas regiones, pero aumentó significativamente (P<0,05) en la zona media del menisco. Los colágenos de tipo I, II y III se distribuyeron en las regiones y zonas de los meniscos. El colágeno tipo I era abundante dentro del menisco. Por el contrario, el colágeno tipo III se localiza principalmente en la zona media. En conclusión, los meniscos felinos exhiben variaciones morfométricas y características histológicas distintivas, lo que ofrece información crucial para veterinarios e investigadores.

PALABRAS CLAVE: Meniscos; Morfometría; Histología; Articulación de la rodilla; Felino.

REFERENCES

Abumandour, M. M.; Bassuoni, N. F.; El-Gendy, S.; Karkoura, A. & El-Bakary, R. Comparative morphological studies of the stifle menisci in donkeys, goats and dogs. *J. Morphol. Sci., 36*:72-84, 2019.

Adams, M. E. & Muir, H. The glycosaminoglycans of canine menisci. *Biochem. J., 197*:385-9, 1981.

Beale, B. *Feline arthroscopy*. Elsevier Science, Amsterdam, 2009.

Bennett, D.; Zainal Ariffin, S. M. & Johnston P. Osteoarthritis in the cat: 1. how common is it and how easy to recognize? *J. Feline Med. Surg., 14*:65-75, 2012.

Braz, PRP, Silva WG (2010) Meniscus morphometric study in humans. *J. Morphol. Sci., 27*:62-6, 2010.

Cengiz, I. F.; Pereira, H.; Pego, J. M.; Sousa, N.; Espregueira-Mendes. J.; Oliveira, J. M. & Reis, R. L. Segmental and regional quantification of 3D cellular density of human meniscus from osteoarthritic knee. *J. Tissue Eng., 11*:1844-52, 2015.

Chakravarthy, D. J. P. & Khanday, D. S. Morphology and morphometry of knee menisci. *Int. J. Curr. Res., 10*:71921-34, 2018.

Chevrier, A.; Nelea, M.; Hurtig, M. B.; Hoemann, C. D. & Buschmann, M. D.Meniscus structure in human, sheep, and rabbit for animal models of meniscus repair. *J. Orthop. Res., 27*:1197-203, 2009.

Denny, H. R. & Butterworth, S. J. A *Guide to Canine and Feline Orthopaedis Surgery*. Wiley-Blackwell, United States, 2000.

Dyce, K. M.; Sack, W. O. & Wensing, C. J. G. *Textbook of veterinary anatomy.* Elsevier Science, Amsterdam, 2017.

Eyre, D. R. & Wu, J. J. Collagen of fibrocartilage: a distinctive molecular phenotype in bovine meniscus. *FEBS Lett 158*:265-70, 1983.

Fedje-Johnston, W.; Tóth, F.; Albersheim, M.; Carlson, C. S.; Shea, K. G.; Rendahl, A. & Tompkins, M. Changes in matrix components in the developing human meniscus. *Am. J. Sports Med., 49*:207-14, 2021.

Fox, A. J.; Bedi, A. & Rodeo, S. A. The basic science of human knee menisci: structure, composition, and function. *Sports Health, 4*:340-51, 2012.

Gupta, G. K.; Kumar, P.; Rani. S. & Kumari, A. Morphological study of the menisci of the knee joint in human cadaver in Jharkhand population. *J. Family Med. Prim. Care, 11*:4723-9, 2022.

Johnson, T. R. & Steinbach, L. S. *Essentials of musculoskeletal imaging.* Elsevier Science, Philadelphia, 2005.

Kale, A.; Kopuz, C.; Edyzer, M.; Aydin, M. E.; Demyr, M. & Ynce, Y. Anatomic variations of the shape of the menisci: a neonatal cadaver study. *Knee Surg. Sports Traumatol. Arthrosc., 14*:975-81, 2006.

Kambic, H. E. & McDevitt, C. A. Spatial organization of types I and II collagen in the canine meniscus. *J. Orthop. Res., 23*:142-9, 2005.

Kim, J. G.; Han, S. W. & Lee, D. H. Diagnosis and treatment of discoid meniscus. *Knee Surg. Relat. Res., 28*:255-62, 2016.

Kim, J. H.; Ahn, J. H.; Kim, J. H. & Wang, J. H. Discoid lateral meniscus: importance, diagnosis, and treatment. J. Exp. Orthop., 7:81, 2020.

Koch, C. & Kornmayer, M. Isolated medial meniscal tear in a domestic shorthaired cat. *Vet. Rec. Case Rep., 2023*:e760, 2023.

Leumann, A.; Leonard, T.; Nüesch, C.; Horisberger, M.; Mündermann, A. & Herzog, W. The natural initiation and progression of osteoarthritis in the anterior cruciate ligament deficient feline knee. *Osteoarthr. Cartil., 27*:687-93, 2019.

Liu, J.; Xu, M. Y.; Wu. J.; Zhang, H.; Yang, L.; Lun, D. X.; Hu, Y. C. & Liu, B. Picrosirius-polarization method for collagen fiber detection in tendons: a mini-review. *Orthop. Surg., 13*:701-7, 2021.

McDevitt, C. A. & Webber, R. J. The ultrastructure and biochemistry of meniscal cartilage. *Clin. Orthop., 252*:8-18, 1990.

Messner, K. & Gao, J. The menisci of the knee joint. Anatomical and functional characteristics, and a rationale for clinical treatment. *J. Anat., 193*:161-8, 1998.

Nakano, T.; Dodd, C. M. & Scott, P. G. Glycosaminoglycans and proteoglycans from different zones of the porcine knee meniscus. *J. Orthop. Res., 15*:213-20, 2005.

Nerurkar, N. L.; Sen, S.; Baker, B. M.; Elliott, D. M. & Mauck, R. L. Dynamic culture enhances stem cell infiltration and modulates extracellular matrix production on aligned electrospun nanofibrous scaffolds. *Acta Biomater., 7*:485-91, 2011.

O'Connor, B. L.; & McConnaughey, J. S. The structure and innervation of cat knee menisci and their relation to a "sensory hypothesis" of meniscal function. *Am. J. Anat., 153*:431-42, 1978.

Parsons, F. G. The joints of mammals compared with those of man: a course of lectures delivered at the Royal College of Surgeons of England. *J. Hum. Anat. Physiol., 34*:41-68, 1899.

Pauli. C.; Grogan, S. P.; Patil, S.; Otsuki, S.; Hasegawa, A.; Koziol, J.; Lotz, M. K.; D'Lima, D. D. Macroscopic and histologic analysis of human knee menisci in aging and osteoarthritis. *Osteoarthritis and Cartilage 19*:1132-41, 2011.

Prosé, L. P. Anatomy of the knee joint of the cat. *Acta Anat. (Basel),119*:40-8, 1984.

Ruthrauff, C. M.; Glerum, L. E. & Gottfried, S. D. Incidence of meniscal injury in cats with cranial cruciate ligament ruptures. Can. Vet. J., 52:1106-10, 2011.

Scott, P. G.; Nakano, T. & Dodd, C. M. Isolation and characterization of small proteoglycans from different zones of the porcine knee meniscus. *Biochim. Biophys. Acta, 1336*:254-62, 1997.

Starke, C.; Lohmann, C. H. & Kopf, S.Stiffness of meniscus tissue depends on the tibiofemoral load and structural integrity of the meniscus root. *J. Med .Eng., 232*:418-22, 2018.

Subramanian, S. & Balakrishnan, A. P. A Study on the morphometry of a medial meniscus in the knee joint of human cadavers in the South Indian population. *Cureus, 15*:e42753, 2023.

Takroni, T.; Laouar, L.; Adesida, A.; Elliott, J. & Jomha, N. Anatomical study: comparing the human, sheep, and pig knee meniscus. *J. Exp. Orthop., 3*:35, 2016.

Vanderploeg, E. J.; Wilson, C. G.; Imler, S. M.; Ling, C .H. & Levenston, M. E. Regional variations in the distribution and colocalization of extracellular matrix proteins in the juvenile bovine meniscus. *J. Anat., 221*:174-86, 2012.

Voss, K.; Karli, P.; Montavon, P. M. & Geyer, H. Association of mineralization in the stifle joint of domestic cats with degenerative joint disease and cranial cruciate ligament pathology. *J. Feline Med. Surg., 19*:27–35, 2017.

Wang, X.; Jing, L.; Wang, X.; Li, Z.; Zhang, Z. & Yang, J. Effects of medial meniscal slope and medial posterior tibial slope on the locations of meniscal tears: a retrospective observational study. *Medicine (Baltimore), 99*:e23351, 2020.

Yan, W.; Dai, W.; Cheng, J.; Fan, Y.; Zhao, F.; Li, Y.; Maimaitimin, M.; Cao, C.; Shao, Z.; Li, Q.; Liu, Z.; Hu, X. & Ao, Y. Histologically confirmed recellularization is a key factor that affects meniscal healing in immature and mature meniscal tears. *Front. Cell. Dev. Biol., 8*:793820, 2021.

Corresponding author:
Dr. Siti Mariam Zainal Ariffin (DVM, PhD)
Faculty of Veterinary Medicine
Universiti Putra Malaysia
43400 UPM Serdang
Selangor
MALAYSIA

E-mail: sitimariam_za@upm.edu.my